Universiteit
Leiden
The Netherlands

Molecular engineering of plant development using Agrobacterium-mediated protein translocation

Khan, M.

Citation
Khan, M. (2017, March 22). *Molecular engineering of plant development using Agrobacterium-mediated protein translocation*. Retrieved from https://hdl.handle.net/1887/47374

Version:	Not Applicable (or Unknown)
License:	Licence agreement concerning inclusion of doctoral thesis in the Institutional Repository of the University of Leiden
Downloaded from:	https://hdl.handle.net/1887/47374

Note: To cite this publication please use the final published version (if applicable).

Cover Page

Universiteit Leiden

The handle http://hdl.handle.net/1887/47374 holds various files of this Leiden University dissertation

Author: Khan, M.
Title: Molecular engineering of plant development using Agrobacterium-mediated protein translocation
Issue Date: 2017-03-22

A GENERIC SPLIT-GFP-BASED REPORTER SYSTEM FOR AGROBACTERIUM-MEDIATED PROTEIN TRANSLOCATION IN PLANTS

4

Majid Khan[1,2], Remko Offringa[1]

[1]Molecular and Developmental Genetics, Institute of Biology Leiden, Leiden University, Sylvius Laboratory, Sylviusweg 72, 2333 BE Leiden, Netherlands
[2]Institute of Biotechnology & Genetic Engineering, The University of Agriculture, Peshawar, 25130, Khyber Pakhtunkhwa, Pakistan

ABSTRACT

Agrobacterium tumefaciens is well characterized for its ability to transfer DNA to plant and fungal cells, but the fact that it also translocates proteins to its host cells was only revealed more recently. *Agrobacterium*-mediated protein translocation (AMPT) was first detected by restoration of a resistance marker or GFP reporter following translocation of a Cre recombinase-VirF/VirE2 protein fusion. Later the split-GFP system was used to detect translocation of GFP_{11}-Vir fusions to recipient reporter lines overexpressing GFP_{1-10}. Unfortunately, these translocation reporter systems are not easily applicable to *Agrobacterium*-mediated transformation (AMT) resistant and regeneration recalcitrant plants such as sweet pepper and tulip, for which the generation of reporter lines are difficult. Here, we designed a generic split-GFP-based reporter system for AMPT to be used directly in wild-type plants. In this system, the GFP_{1-10} part is transiently expressed from a T-DNA that is co-transferred with a fusion protein comprising the GFP_{11} part and the C-terminal translocation signal of VirF from the same *Agrobacterium* to any desired wild-type recipient cell. This modified generic protein translocation reporter system was successfully tested in a variety of tissues of different plant species, such as *Nicotiana benthamiana*, *Nicotiana tabacum*, *Arabidopsis thaliana*, *Capsicum annum* and *Tulipa gesneriana*. The system reported efficient AMPT to these plant species, and also appeared to be useful for optimization of AMT of tulip, and for the visual selection of transgenic tulip shoots.

Keywords: *Agrobacterium tumefaciens*, Protein translocation, Split-GFP, Generic system, Tulip

INTRODUCTION

The soil born gram negative plant pathogenic bacterium *Agrobacterium tumefaciens* is the most common and successful tool for plant transformation (Ziemienowicz, 2014). The capacity of *A. tumefaciens* to transfer DNA to plant cells is determined by an extrachromosomal circular DNA molecule called tumor inducing (Ti) plasmid, which the bacterium normally uses to induce crown gall tumors on its host plants (Larebeke et al., 1974). After the discovery that the crown gall disease was caused by transfer of a copy of a specific region of the Ti plasmid, the transfer or T-region, to the host cells, *A. tumefaciens* became a tool for plant transformation (Ziemienowicz, 2014).

The process of *Agrobacterium*-mediated DNA transfer starts with the induction of genes in the *vir*-region on the Ti plasmid by signaling molecules exuded by wounded plant tissues (Subramoni et al., 2014). Phenolic compounds, such as acetosyringone, are the most potent inducers of *vir* gene expression in wounded plant exudates (Stachel et al., 1985). Other signals, such as temperature, low pH and certain aldose-type monosaccharides, can enhance *vir* gene induction (Melchers et al., 1989). All these signals are perceived by the transmembrane receptor VirA (Melchers et al., 1989), which subsequently activates the transcriptional regulator VirG through a typical bacterial two-component phosphorylation system (Jin et al., 1990). VirG subsequently activates the transcription of the *vir* operons, resulting in the production of 11 VirB proteins that together with VirD4 assemble into the type-4 secretion system (T4SS) translocation pilus (Chandran Darbari and Waksman, 2015). The VirB proteins make up the T-pilus through which T-DNA and Vir proteins are translocated into the host cell, while VirD4 acts as a coupling protein that recognizes DNA and proteins that are to be translocated (Lai and Kado, 2000; Kumar and Das, 2002; Zupan et al., 2007). Among the Vir proteins, VirD1 and VirD2 form a relaxase that introduces a nick in the bottom strand of the Ti plasmid at the position of imperfect border repeats that delineate the T-region (Wang et al., 1987; Vogel and Das, 1992). During this nicking, VirD2 becomes covalently attached to the 5′ end of the single stranded T-DNA where it serves to recruit and guide the T-DNA during translocation by the T4SS to the nucleus of the host cell (Lacroix et al., 2006). By using a Cre recombinase Reporter Assay for Translocation (CRAfT) it was demonstrated that the T4SS system can also mediate transfer of Vir proteins, such as VirE2 and VirF, to the host cells independent of the T-DNA, and that the signal peptide responsible for protein translocation is located in the C-terminal part of these Vir proteins (Vergunst et al., 2000). The function of these translocated Vir proteins is to maintain the integrity of T-DNA inside the host cell and help its integration in the host genome (Lacroix and Citovsky, 2013).

Detection of protein translocation by the CRAfT system involved Cre-Vir fusion protein-mediated excision of a *lox*-flanked (floxed) DNA segment that disrupted a kanamycin resistance selection marker or a *GFP* reporter gene (Vergunst et al., 2000; Vergunst et al., 2005). However, the CRAfT system did not allow to follow translocated proteins in the recipient cells. As GFP-VirF or GFP-VirE2 fusions were not translocated by the *Agrobacterium* T4SS, probably because of the complex structural folding of the GFP protein (Vergunst et al., 2005), the split-GFP system was adapted for visualization of *Agrobacterium*-mediated protein translocation (AMPT) (Li et al., 2014; Sakalis et al., 2014). This split-GFP system was specifically developed to detect protein

translocation by the type III secretion system (T3SS) of *Salmonella enterica* into human cells (Van Engelenburg et al., 2010). Adaptation of this system for the visualization of AMPT to yeast and plant cells involved expression of GFP_{11}-Vir fusion proteins in *Agrobacterium* cells and generation of yeast or plant reporter lines that stably express the complementary GFP part (GFP_{1-10}) in the recipient cells (Li et al., 2014; Sakalis et al., 2014). Upon its translocation to recipient cells, the GFP_{11}-Vir fusion will recreate a functional GFP protein by interacting with the GFP_{1-10} part in the reporter line and thus result in fluorescent signals (Sakalis et al., 2014).

Visualization of AMPT is not only important for fundamental studies on the bacterial protein translocation process itself, but also for application of AMPT to check the efficiency of protein translocation, and whether the protein of interest is correctly localized in the target recipient cells. One drawback of the split-GFP system is that the recipient organism must be transformed *a priori* with a construct that expresses the GFP_{1-10} part. Especially for transformation resistant or regeneration recalcitrant plants this step can be time consuming and difficult. Here we report on the construction of a new generic split-GFP system for visualization of AMPT in wild-type plants. In the new system the GFP_{1-10} part and the GFP_{11} part are delivered into the host cell from the same *Agrobacterium* strain, with GFP_{1-10} expressed from the T-DNA following *Agrobacterium*-mediated transformation (AMT) and GFP_{11} as part of a Vir protein fusion by AMPT. The GFP_{1-10} coding region was modified with an intron sequence (Pang et al., 1996) to prevent GFP_{1-10} expression in *Agrobacterium*. Using this new generic reporter system we successfully visualized AMPT in a variety of tissues from different plant species, among which the recalcitrant crop species *Capsicum annuum* and *Tulipa gesneriana*.

RESULTS

Testing *GFP-intron* versions and *Agrobacterium* strains in tobacco leaf infiltration

As a first step in developing a generic split-GFP system for visualization of AMPT, we verified that the GFP version that was originally used for the split-GFP assays (GFP) was sufficiently bright by comparing it to the previously reported plant-enhanced GFP (pGFPi) version (Pang et al., 1996). The *pGFPi* coding sequence was disrupted by the *intron IV* sequence of the potato *ST-LS1* gene introduced at a splicable position (Pang et al., 1996). Synthetic intron-containing coding regions *GFP(i)* and *pGFP(i)* placed on a T-DNA under control of the *CaMV 35S* promoter were introduced into *A. tumefaciens* strains LBA1100 and AGL1. As expected, the intron-containing reporters *p35S::GFP(i)* and *p35S::pGFP(i)* did not lead to GFP expression in *Agrobacterium* (Fig. S1). When the resulting strains were used to infiltrate intact leaves on *N. benthamiana* plants, there was no obvious difference in the number of plant cells that showed GFP expression or the intensity of the GFP fluorescence (Fig. 1 a and b). As this indicated that both constructs were equally suited as transformation reporter, we continued to use the *GFP(i)* gene construct for our experiments. A comparison of *A. tumefaciens* strains AGL1 *35S::GFP(i)* and LBA1100 *35S::GFP(i)* in *N. benthamiana* and *N. tabacum* leaf infiltration experiments showed that the super virulent AGL1 strain was more efficient in AMT than LBA1100 (Fig. 1c and d). The absence of green fluorescence in leaves infiltrated with the *virD4* mutant strain

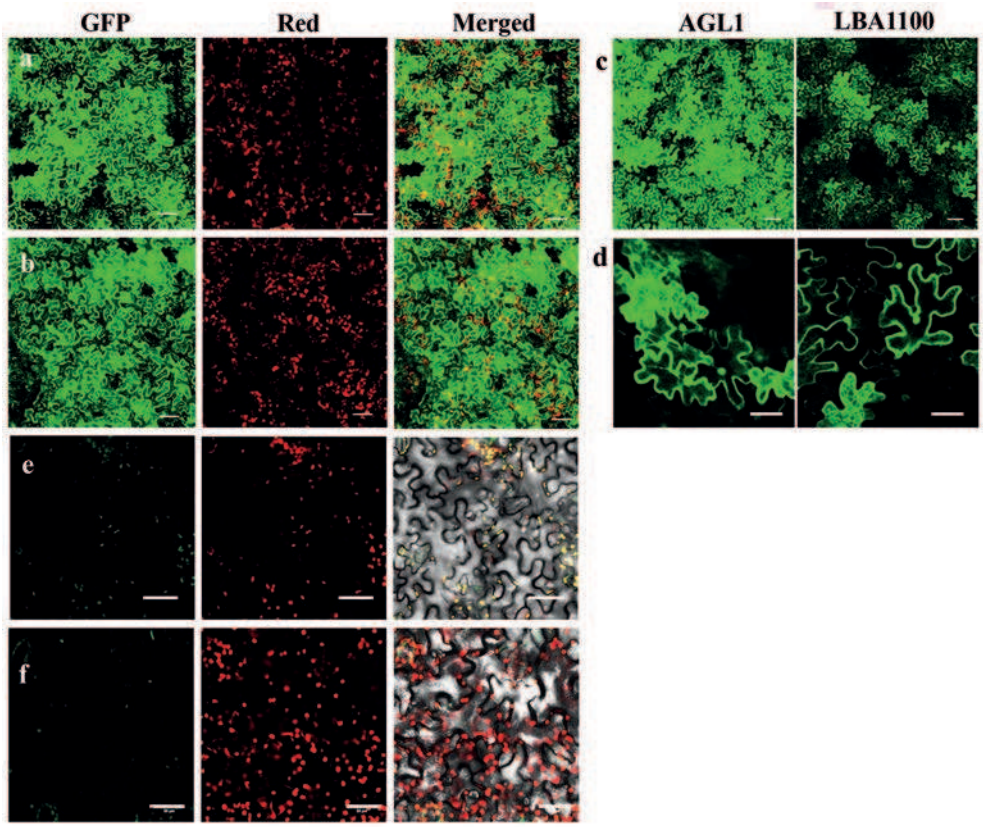

Figure 1. Comparison of AMT efficiencies using different *Agrobacterium* strains and GFP-intron versions in tobacco leaf infiltration experiments. a-f) Representative confocal laser scanning microscopy images of *Nicotiana benthamiana* (a, b, c, e) or *Nicotiana tabacum* (d, f) leaf tissues 3-4 days after infiltration with *Agrobacterium* strains AGL1 *p35S::GFP(i)* (a, c and d left panel), AGL1 *p35S::pGFP(i)* (b), LBA1100 *p35S::GFP(i)* (c and d right panel) or LBA2587 (*virD4* deletion mutant) *p35S::GFP(i)* (e, f). Left, middle and right panel in (a, b, e, f) show GFP channel, red channel and merged image of GFP, red and transmitted light channels, respectively. GFP channel images are shown in (c, d). Scale bar is 0.1 mm.

LBA2587 (Sakalis et al., 2014) containing *35S::GFP(i)* (Fig. 1e and f) showed that the GFP signals observed with the other strains were the result of AMT.

Construction of a generic split-GFP system for visualization of AMPT

After the confirmation that the *35S::GFP(i)* construct was an effective reporter in plant cells, we modified the original split-GFP system (Fig. 2a) (Sakalis et al., 2014) by generating an intron-containing version of GFP_{1-10}. In addition, we fused a nuclear localization signal (NLS) to the N-terminus of the GFP_{1-10} part, as we expected that nuclear accumulation would facilitate the detection of the generally weak fluorescent signals in the nuclei after AMPT. The resulting plasmid *35S::NLS-*GFP_{1-10}*(i)* was introduced into *Agrobacterium* strain AGL1 already containing construct *pvirF::*GFP_{11}*-dvirF*. In this bacterium, expression of the GFP_{11} part fused to the 50

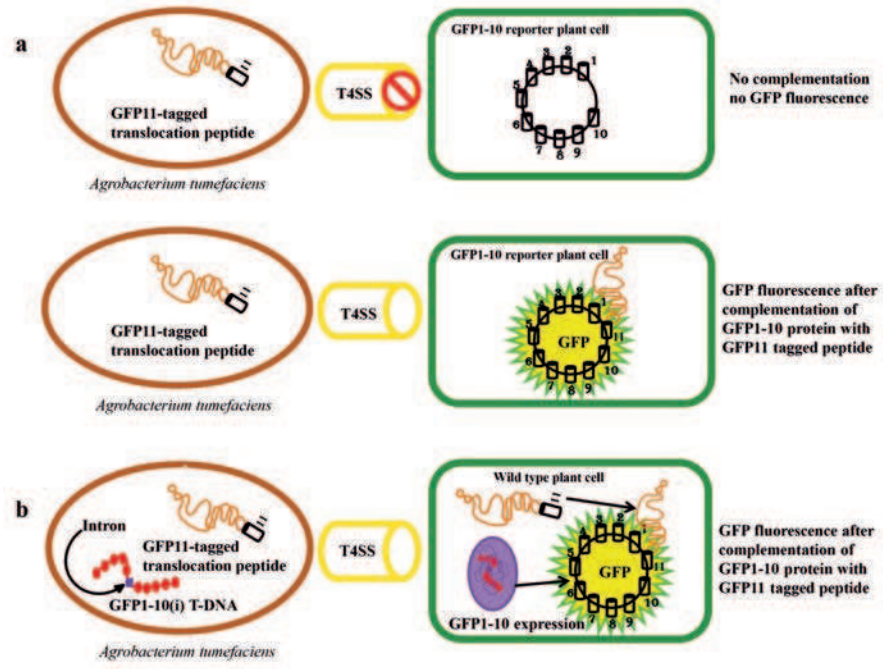

Figure 2. A schematic representation of the original and the generic split-GFP-based reporter system for AMPT in plant cells. a) The original split-GFP system for visualization of AMPT. *Agrobacterium tumefaciens* strains AGL1 *pVirF::GFP*$_{11}$*-dVirF* (lower) and LBA2587 (VirD4 mutant) *pViF::GFP*$_{11}$*-dVirF* (upper) both express a GFP$_{11}$-tagged protein fused with the C-terminal VirF translocation signal. Strain LBA1143 will not translocate the fusion protein because it lacks a functional T4SS, and therefore no GFP$_{1-10}$ complementation and GFP fluorescence will be observed in cells of the GFP$_{1-10}$ reporter plant line (upper). Translocation of the GFP$_{11}$-protein-VirF fusion by the AGL1 strain will result in complementation of GFP$_{1-10}$ in the recipient GFP$_{1-10}$ reporter plant cells that thus become green fluorescent (b). In the new generic split-GFP-based reporter system *Agrobacterium* strain AGL1 containing *pVirF::GFP*$_{11}$*-dVirF* and *35S::GFP*$_{1-10}$*(i)* will translocate both the T-DNA containing the *35S::GFP*$_{1-10}$*(i)* gene (with a splicable intron (i)) and the GFP$_{11}$-tagged fusion protein to cells of wild-type plants. The translocated GFP$_{11}$-tagged fusion protein will complement the partial GFP$_{1-10}$ protein that is expressed from the T-DNA in the plant cell nucleus, thus leading to GFP fluorescence.

C-terminal amino acids of VirF (dVirF) was controlled by the *virF* promoter. Cocultivation with this *Agrobacterium* strain should only result in GFP positive cells if both the *35S::NLS-GFP*$_{1-10}$*(i)* T-DNA and the GFP$_{11}$-dVirF fusion are translocated to the same plant cell (Fig. 2b). This modified split-GFP system was tested by infiltrating leaves of *Nicotiana benthamiana, Nicotiana tabacum* and *Arabidopsis thaliana* (Fig. 3). For all three plant species the generic split-GFP system allowed us to detect successful AMPT to leaf epithelial cells, but surprisingly in *Arabidopsis* no nuclear GFP signals were observed, even in cells expressing the NLS-GFP(i) protein. This suggests that GFP fusions are inhibited or not able to cross the nuclear pore in *Arabidopsis* (Fig. 3d-f). In contrast, simultaneous expression of the NLS-GFP$_{1-10}$ fusion protein and translocation of GFP$_{11}$-dVirF resulted in a strong fluorescent signal in nuclei of the recipient cells in tobacco plants, indicating that NLS-GFP$_{1-10}$ was able to efficiently recruit the complementing

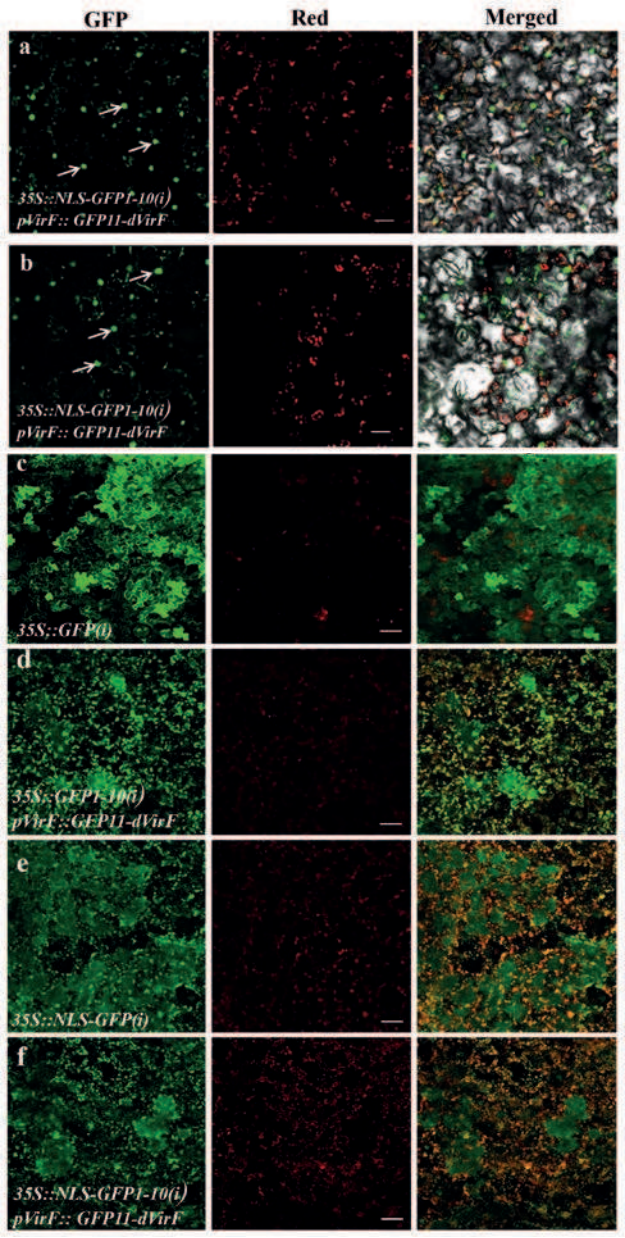

Figure 3. Visualization of AMPT using the new generic split-GFP system in leaves of wild-type tobacco and *Arabidopsis* plants. a,b) Representative confocal laser scanning microscopy images of *Nicotiana benthamiana* (a) and *Nicotiana tabacum* (b) leaf tissues 3-4 days after infiltration with *Agrobacterium* strain AGL1 containing *pVirF::GFP*$_{11}$*-dVirF* and *35S::NLS-GFP*$_{1-10}$*(i)*. c-f) Representative confocal laser scanning microscopy images of *Arabidopsis thaliana* leaf tissues 3-4 days after infiltration with *Agrobacterium* strain AGL1 containing *35S::GFP(i)* (c), *pVirF::GFP*$_{11}$*-dVirF* and *35S::GFP*$_{1-10}$*(i)* (d), *35S::NLS-GFP(i)* (e) and *pVirF::GFP*$_{11}$*-dVirF* and *35S::NLS-GFP*$_{1-10}$*(i)* (f). Left, middle and right panel in (a-f) show the GFP channel, the red channel and a merged image of the GFP, red and transmitted light channels, respectively. Arrows indicate GFP fluorescent nuclei. Scale bar is 0.1 mm.

GFP_{11} part to the nucleus. This nuclear localization enabled us to easily score the number of GFP positive cells and calculate and compare AMPT and AMT efficiencies (see below).

Optimization and efficiency of the new generic split-GFP system

A disadvantage of the new generic split-GFP-based reporter system for AMPT is that both components are located on separate plasmids that are maintained in *Agrobacterium* by antibiotic selection. Since the bacteria are not under antibiotic selection during the infiltration/cocultivation period, plasmids might be lost, leading to a reduced efficiency of T-DNA and/or protein translocation. To simplify the new generic split GFP system and possibly also to enhance the efficiency of this new system, we generated a single plasmid containing both the *p35S::NLS-GFP$_{1-10}$(i)* and the *pvirF::GFP11-dvirF* part. Protein translocation via this 'fused' generic split-GFP system was confirmed through *N. benthamiana* leaf infiltration (Fig. 4c). In the same experiment we also infiltrated *N. benthamiana* leaves with strain AGL1 *35S::NLS-GFP(i)* to monitor AMT efficiency, and with strain AGL1 containing *p35S::NLS-GFP$_{1-10}$(i)* and *pvirF::GFP11-dvirF* to monitor AMPT from the separate system (Fig. 4a,b). Quantification of the percentage of fluorescent recipient cells showed that there was no significant difference between AMPT via the separate or fused generic split-GFP system, while AMT resulted in two-fold more GFP positive nuclei (Fig. 4d). This difference between AMT and AMPT might relate to the fact that in the case of AMPT two components have to be translocated simultaneously to the recipient plant cell. Alternatively, the possibly low number of translocated GFP_{11} proteins might limit the detection of protein translocation in some of the recipient plant cells.

AMPT of potential regeneration-enhancing proteins to *Capsicum annuum*

Capsicum annuum (sweet pepper) is regarded as one of the crop plants that is most recalcitrant to AMT (Kotharet al., 2010). Previously, it was shown that DEX-mediated activation of a BABY BOOM-Glucocorticoid Receptor (BBM-GR) fusion protein enabled the selection of transgenic shoots after AMT by enhancing the shoot regeneration process (Heidmann *et al.*, 2011). A disadvantage of this method is that first a transgenic line with the *35S::BBM-GR* construct has to be generated that can subsequently be used for AMT by BBM-enhanced regeneration of transgenic shoots. Here we tested the possibility of AMPT of BBM and AT-HOOK CONTAINING NUCLEAR PROTEIN-LIKE 15 (AHL15) to tissues of *C. annuum.* In Chapter 3 we showed that both of these proteins enhanced shoot regeneration from tobacco leaf discs. If successful, this would allow the use of AMPT as an alternative method to enhance regeneration and selection of transgenic *C. annuum* plants. Our new generic split-GFP reporter system was used to visualize the translocation of GFP_{11}-BBM-VirF or GFP_{11}-AHL15-VirF fusion proteins to *C. annuum* cells. Cotyledon explants were syringe infiltrated with *Agrobacterium* strain AGL1 containing either the *pvirF::GFP$_{11}$-virF*, *pvirF::GFP$_{11}$-BBM-virF* or *pvirF::GFP$_{11}$-AHL15-virF* construct together with the *35S::NLS-GFP$_{1-10}$(i)* T-DNA construct on another plasmid. Confocal microscopy of the infiltrated cotyledon tissues showed nuclear GFP signals in the epithelial cells for all three *Agrobacterium* strains (Fig. 5), indicating successful AMPT. Because the background fluorescence was quite high, it was difficult to determine the efficiency of AMPT in *C. annuum*. Although we did not score for an immediate positive effect on shoot

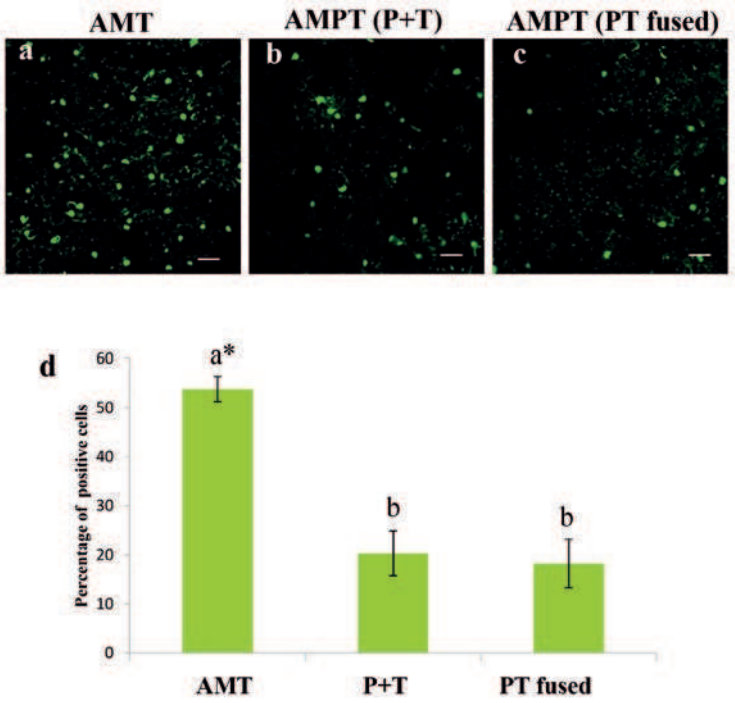

Figure 4. The efficiency of AMT in infiltrated tobacco leaves is two-fold higher compared to AMPT. a-c) Representative confocal laser scanning microscopy images of wild-type *Nicotiana benthamiana* leaves three days after infiltration with *Agrobacterium* strain AGL1 containing *35S::NLS-GFP(i)* for detection of AMT (a), or AGL1 *35S::GFP*$_{1\text{-}10}$*(i)* with *pVirF::GFP*$_{11}$*-dVirF* (P+T, b)), or AGL1 *35S::GFP*$_{1\text{-}10}$*(i)-pVirF::GFP*$_{11}$*-dVirF* (PT fused, c) for detection of AMPT. Scale bar is 0.1mm. d) Graph showing the AMT or AMPT (P+T or PT fused) efficiencies as percentage of positive cells. The efficiency was calculated based on the number of GFP-positive nuclei over the total number of nuclei in a single image. Bars represent average percentages determined from confocal images from three different parts of three leaves (n =9) of an infiltrated plant. Error bars depict the SEM. Significantly different values are differently labeled with a and b (Post ANOVA Tukey's test, $p<0.05$).

regeneration in our experiments, these results show that our new generic split-GFP-based reporter system can be used in crop plants to optimize the conditions for enhanced selection and regeneration of transgenic plants by combined AMPT and T-DNA delivery.

Successful protein translocation and T-DNA transfer to tulip cells

The AMT of monocot plant species is generally more difficult than that of dicot plant species. Different methods other than *A. tumefaciens* transformation can be used, such as the gene gun, but generally these result in lower transformation efficiencies (Barampuram and Zhang, 2011). After confirmation and successful application of the GFP(i)-based generic split-GFP AMPT reporter system in tobacco and *C. annuum*, it was also applied on one of the most recalcitrant monocot species *Tulipa gesneriana* (tulip). DNA transformation to tulip has previously been reported, but with low efficiency (Wilmink et al., 1992). Based on these results, we expected to see only low AMPT efficiencies in tulip using the generic split-GFP reporter system. To our

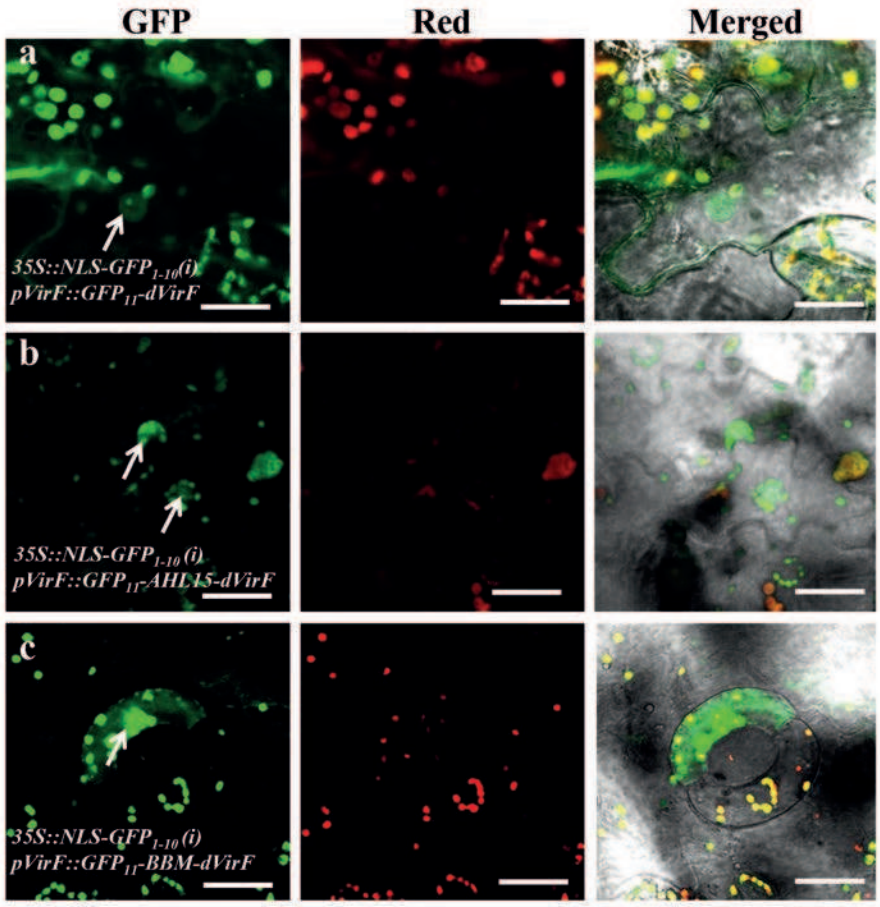

Figure 5. Visualization of AMPT of plant developmental regulators to *Capsicum annuum* cotyledon cells using the generic split-GFP system. a-c) Syringe infiltrated cotyledons of *Capsicum annuum* visualized under a confocal microscope after 3 days of cocultivation with *Agrobacterium* strain AGL1 containing *35S::NLS-GFP$_{1-10}$(i)* along with either construct *pVirF::GFP$_{11}$-dVirF* (a), *pVirF::GFP$_{11}$-AHL15-dVirF* (b) or *pVirF::GFP$_{11}$-BBM-dVirF* (c). GFP fluorescent nuclei of the recipient cells are indicated by arrows. Left panel shows the GFP channel, middle panel shows the autofluorescence in the red channel, and right panel shows the merged image of the green, red and transmitted light channels. Scale bare is 30μm.

surprise, however, nuclear GFP fluorescence was observed at an unexpectedly high efficiency either after AMT or after AMPT, especially in vertically cut thin layer sections of regenerated shoot explants (Fig. 6a,b). These results of T-DNA and protein translocation to tulip cells stimulated us to investigate possibilities to optimize the protocol for genetic modification of this economically important plant species.

As there is no standard protocol available yet for the *Agrobacterium*-mediated transformation of tulip, we performed a time-lapse experiment where the optimum duration of co-cultivation was investigated by multiple observations using confocal laser scanning microscopy. *In vitro* tulip tissues were co-cultivated for up to 9 days with the *Agrobacterium* strain AGL1 containing

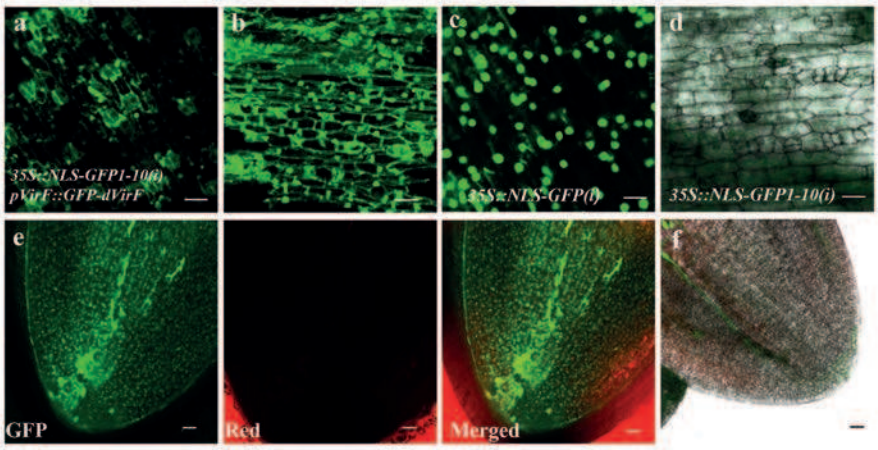

Figure 6. Visualization of AMPT and stable AMT in tulip cells. a,b) Representative confocal laser scanning microscopy images of transverse (a) or vertical (b) sections of tulip explants after 7 days of cocultivation with *Agrobacterium* strain AGL1 containing *35S::GFP*$_{1-10}$*(i)* and *pVirF::GFP*$_{11}$*-dVirF* to detect AMPT. The transverse section shows GFP fluorescence in nuclei of the cells and also in stomatal cells (a), while in the vertical section most of the nuclei are brightly fluorescent along with cytosolic signals (b). c,d) Confocal laser scanning microscopy images of transverse sections of tulip explants after 7 days of cocultivation with *Agrobacterium* strain AGL1 *35S::NLS-GFP(i)* to detect AMT (c) or with AGL1 *35S::NLS-GFP*$_{1-10}$*(i)* as negative control (d). e,f) Representative confocal laser scanning microscopy images of regenerated tulip shoots 4-5 weeks after cocultivation with AGL1 *35S::NLS-GFP(i)* (e), or with negative control strain AGL1 *35S::NLS-GFP*$_{1-10}$*(i)* (f). (Left, middle and right panels in (e) show the GFP channel, the red channel, and a merged image of the GFP and red channel while pannel (f) shows a merged image of GFP, red and transmitted light channels, respectively). Scale bar in all images is 0.1mm.

35S::NLS-GFP$_{1-10}$*(i)* and *pvirF::GFP*$_{11}$*-dvirF*. The tulip tissues were observed at different time points (5, 7 and 9 days). The results showed increased GFP fluorescence after 7 days of co-cultivation (Fig. S2). Extending the co-cultivation period up to 9 days resulted in overgrowth of bacteria and in tissue necrosis accompanied by high autofluorescence, which interfered with observation of GFP signals. The optimized conditions of 7 days co-cultivation of tulip explants on hormone free MS medium with 40mg/L acetosyringone, resulted in enhanced protein translocation, whereas longer co-cultivation damaged the explant tissues as a result of the bacterial overgrowth. Strikingly, the use of growth hormone containing medium with acetosyringone during co-cultivation prevented this overgrowth of *Agrobacteria* for up to two weeks, but resulted in reduced AMPT efficiencies, most likely because the proliferating cells on hormone medium produced antibacterial compounds that prevented *Agrobacterium* growth.

In the time lapse experiments we also infiltrated tulip tissues with *A. tumefaciens* containing *35S::NLS-GFP(i)* for T-DNA transfer as positive control. After 7 days of co-cultivation, some of the tissues were transferred to hormone containing medium without selection. Some of the regenerated shoots obtained after 4-5 weeks on this medium showed nuclear GFP signals in all cells (Fig. 6e), suggesting stable integration and expression of *35S::NLS-GFP(i)*. DAPI staining confirmed that the observed GFP signals were located in the nuclei of tulip cells (Fig. S3). Although, the regeneration efficiency of tulip varies per explant, these experiments

showed that efficient AMPT and AMT can be achieved in tulip by using the *35S::NLS-GFP(i)* construct as a reporter for stably transformed regenerating shoots. These first results pave the way for the establishment of a stable AMT system for tulip.

DISCUSSION

Previous studies have shown that the most acceptable tool for generating transgenic plants, *Agrobacterium tunefaciens*, can also be used to translocate desired proteins into plant or yeast cells (Vergunst et al., 2000; Schrammeijer et al., 2003). Two reporter systems have been developed to study and optimize this AMPT, but until now these methods relied on the construction of stably transformed reporter lines, either containing a marker gene disrupted by a floxed insert to detect translocation of the Cre recombinase, or a split-GFP-based system where a stable line is generated that expresses the non-fluorescent GFP_{1-10} to detect translocation of the complementing GFP_{11} part (Li et al., 2014; Sakalis et al., 2014). The advantage of the latter system is that it allows to follow the translocated protein in the recipient cells to its predominant final localization (Li et al., 2014; Sakalis et al., 2014). Here we generated a generic split-GFP-based reporter system for direct visualization of AMPT in wild-type recipient cells. The advantage of this generic split-GFP system is that both the GFP_{1-10} and the GFP_{11} parts are transferred by the same *Agrobacterium* strain, thereby circumventing the time consuming step to generate a GFP_{1-10} expressing reporter line, but also to make the method applicable to transformation resistant plants species. This new generic split GFP system has been successfully used to show AMPT to cells of tobacco and *Arabidopsis*, and to the transformation recalcitrant crops sweet pepper and tulip.

Using the original version of split-GFP, most of the observed GFP signals localized to the cytosol of the plant cells (Sakalis *et al.*, 2014; Chapter 3). The cytosolic signals were generally weak and difficult to score because they were hard to distinguish from background fluorescence. To avoid this problem, a nuclear localization signal (NLS) was added to the GFP_{1-10} moiety. Using this, we could show that AMPT is only 2-fold less efficient than AMT, which is still surprisingly high in view of previously published efficiencies (Sakalis et al., 2014). One has to keep in mind, however, that the observed AMPT efficiency is likely to be an underestimation, since detection of AMPT with the generic system requires translocation of both T-DNA and protein and might be limited by the number of GFP_{11}-dVirF fusion proteins translocated. Having the *35S::NLS-GFP_{1-10}(i)* and *pvirF::GFP_{11}-dvirF* parts at separate or at one construct did not change the AMPT efficiency. However, in some tissue explants we even obtained more GFP positive cells with AMPT than with AMT, suggesting that infiltration handling, leaf tissue damage and tissue type also considerably contribute to the AMPT efficiency, and that in fact the AMT and AMPT efficiencies do not differ that much.

Application of our new generic split-GFP-based AMPT reporter system to the AMT resistant crops sweet pepper and tulip showed that both crop species are not resistant to AMT or AMPT, but rather that efficient regeneration of the transformed cells into transgenic plants is problematic. For sweet pepper this was already reported previously (Heidmann et al., 2011), but for tulip the high AMT and AMPT efficiencies came as a surprise. For sweet pepper, usually cotyledon explants are used for AMT (Heidmann et al., 2011), and by applying our syringe infilteration

technique on these tissues, we observed many cells with GFP signals in both the nucleus and cytosol. However, due to the sensitivity of the sweet pepper tissues to *Agrobacterium*-infiltration induced necrosis, the high intensity of autoflourescence made it also difficult to detect GFP signals. Our results showed that it is possible to introduce regulatory proteins, such as BBM and AHL15, to sweet pepper cells via AMPT, and besides the enhancement of regeneration, as has been shown for BMM in sweet pepper (Heidmann et al., 2011), this method could be used to translocate proteins that reduce the tissue necrosis reaction.

Tulip inflorescence stem explants harvested from bulbs appeared to be relatively insensitive to cocultivation with *Agrobacterium*, and leaving the co-cultivation at hormone free medium for an extended period of 7 days led to high AMT and AMPT efficiencies. Subsequent transfer to hormone-containing medium not only started the regeneration, but at the same time induced the production of some anti-bacterial activity that prevented tissue overgrowth by *Agrobacterium*. This has been reported previously for *Centella asiatica* (Bibi et al., 2011). Explants co-cultivated with the AGL1 *35S::NLS-GFP(i)* strain produced homogenous GFP positive shoots after 4 to 5 weeks on hormone medium, suggesting that it is possible to obtain stably transformed tulip plants without selection, purely based on GFP visualization. Our results indicate that this new generic split-GFP system can not only be used to report AMPT, but also to optimize the co-cultivation and tissue culture conditions to efficiently generate and obtain mutant or transgenic lines from plant species that are currently considered to be recalcitrant to AMT or AMPT.

MATERIAL AND METHODS

Bacterial strains and media

Agrobacterium tumefaciens strains are listed in Table 1. All strains were grown in LC medium (10 g/l tryptone, 5 g/l yeast extract and 8 g/l NaCl, pH 7.5) containing (if required) rifampicin, (rif, 20 µg/ml), spectinomycin, (spc, 250 µg/ml), carbenicillin, (cb, 75µg/ml) gentamicin (gent, 40 µg/ml) and kanamycin (km, 100 µg/ml). Ten ml cultures were inoculated with a single colony and incubated under continuous shaking (180 rpm) in 200 ml flasks for two days in an incubator at 30˚C. 10-20 ng of plasmids DNA was electroporated into 50 µl electrocompetent cells (Den Dulk-Ras and Hooykaas, 1995; McCormac et al., 1998) of *A. tumefaciens* strains LBA1100 (Beijersbergen et al., 1992) and AGL1 (Lazo et al., 1991) using prechilled cuvettes and by applying electric pulse at 12.5 kv/cm with a constant time of approximately 4.7 msec (Mersereau et al., 1990). For cloning *Escherichia coli* strain DH5α was used and grown at 37°C in LC medium containing (if required) 100 µg/ml cb, 25 µg/ml gent, and 25 µg/ml km.

Plant material

The plant lines used in this study were: *Nicotiana tabacum* streptomycin resistance-1 (SR-1), *Nicotiana benthamiana, Arabidopsis thaliana* Col-0, *Capsicum annuum* (Bruinsma wonder and Fire flame) and tulip cultivar 'Strong Gold'. *Arabidopsis* seedlings and tulip bulb explants were cultured at 21°C, 50% relative humidity and at 16 hours photoperiod. Nicotiana and Capsicum plants were grown at 25°C, 50% relative humidity and 16 hours photoperiod.

Table 1. List of *Agrobacterium* strains used in this study for *Agrobacterium* infiltration.

Strains	Chromosomal background	Antibiotic resistance	Source
AGL1	C58	rif cb	Jin et al., 1987
LBA1100	C58	rif spc	Beijersbergen et al., 1992
LBA2587(*ΔvirD4*)	C58	rif spc	(Sakalis et al., 2014)

rif: rifampicin; spc: spectinomycin; cb: carbenicillin; Δ: deletion.

Agro-infiltration and co-cultivation

Agrobacterium strains were grown in LC medium as described above and subsequently diluted in AB-sucrose minimal medium containing appropriate antibiotics and grown for overnight at 30°C. Bacterial cultures were induced at gentle rotation (50rpm) and room temperature for 14-24 hours by adding 3,5-dimethoxy-4-hydroxy-acetophenone (acetosyringone AS) [Sigma Aldrich] dissolved in dimethyl sulfoxide (DMSO) to a final concentration of 100μM, as described (Gelvin et al ,2006). Fifteen days old *Arabidopsis* seedlings were infiltrated with the bacterial culture (OD_{600} 0.6) using vacuum infiltration (Rossi *et al.*, 1993) or bacterial cultures were directly injected (Wroblewski et al., 2005) into leaves using a blunt tipped plastic 10 ml syringe (Nissho NIPRO Europe N.V., Zaventem, Belgium). *N. tabacum* and *N. benthamiana* non-sterile leaves of 3-4 weeks old soil grown plants were syringe infiltrated with bacterial cultures of OD_{600} 0.6-0.8. *N. tabacum* surface sterilized leaf discs (Baltes et al., 2014) and *C. annuum* cotyledons from 2 weeks old *in vitro* grown seedlings were also syringe infiltrated (Fig. S4) with bacterial cultures of OD_{600} 0.3-0.4, in the sterile environment of a down flow laminar flow hood and cultivated for 3 days on 40mg/L AS containing MS medium. The tulip tissues were inoculated with AS-induced bacterial culture of OD_{600} 0.6 for overnight in the dark and, after wiping excess bacteria with sterile tissue paper, co-cultivated for up to 9 days on 40mg/L AS containing hormone free MS medium at 21°C, 50% relative humidity.

Leaf samples of *N. tabacum, N. benthamiana* and *A. thaliana* were analyzed 3-4 days after infiltration while tulip samples were analyzed at day 5, day 7 and day 9 of co-cultivation period. For DAPI staining samples were incubated for one hour in 1 mg/l DAPI solution.

Tulip transformation

The sterile tulip bulb (Podwyszyńska and Sochacki, 2010) stem explants (10-12 mm thick), pre-cultured for 3-4 weeks on MS medium supplemented with 1mg/l thidiazuron (TDZ) and 1mg/l 1-naphthalene acetic acid (NAA), were cut into 2-3 mm thin layer explants. After bacterial inoculation and 7 days of co-cultivation (as described above) on hormone free MS medium the explants were transferred back to the pre-culture medium for shoot induction. After 4-5 weeks the regenerated shoots were analyzed for transformation.

Microscopy

All fluorescent microscopy was performed using a Zeiss Imager M1 or a Zeiss observer confocal laser scanning microscopy (CLSM) both equipped with an LSM 5 Exciter scanning module

(Zeiss, Oberkochen, Germany) and 10x, 20x and 40x objectives (numerical aperture 1, 0.8 and 0.65, respectively). GFP signals were detected using an argon 488 nm laser and a 505-530 nm band pass (BP) emission filter. Chloroplast- and other auto-fluorescence were detected using a 650 nm long pass (LP) emission filter following excitation at 488 nm. DAPI was excited using a 405 nm diode laser and emission detected using a 420-480 nm (blue) BP filter.

Plasmid construction

All plasmids used in this study are listed in Table 2. For the T-DNA transfer a modified version of the plasmid pSDM3764 was used which harbors a GFP_{1-10} sequence under control of the *35S CaMV* promoter and the *35S CaMV* terminator (Sakalis et al., 2014). For the intron splicing validation and GFP sequence fluorescence comparison, synthetic fragments (Eurofin) of the full length original GFP (*GFP(i)*) and a plant enhanced full length GFP (*pGFP(i)*) (Appendix 1) coding sequences, containing a splicable 84 nucleotide *intron IV* sequence of the potato *ST-LS1* gene (Pang et al., 1996), were ligated into the *Bst*EII and *Nco*I digested pSDM3764 vector backbone, thereby replacing the GFP_{1-10} sequence (Cabantous et al., 2005) and generating *p35S::GFP(i)* (pSDM6506) and *p35S::pGFP(i)* (pSDM6505). For the new generic split-GFP system, synthetic fragments (Eurofin) containing the GFP_{1-10}*(i)* sequence harboring the intron with and without *NLS* (Appendix 2) were cloned into *Bst*EII and *Nco*I digested pSDM3764, thereby generating *p35S::NLS-*GFP_{1-10}*(i)* (pSDM6509) and *p35S::*GFP_{1-10}*(i)* (pSDM6508). For the translocation of fusion proteins a modified version of the plasmid pSDM3760 (Sakalis et al., 2014) was used, containing the GFP_{11} coding region under the *virF* promoter and fused to the N-terminal part of *dvirF* (Chapter 3). Additionally, for AMPT of plant developmental regulators AHL15 and BBM, *AHL15* and *BBM* coding regions were cloned as translational fusions between GFP_{11} and *dvirF* (Table 2). All cloning steps were performed in *E.coli* strain DH5α (Bethesda Research Laboratories, 1986). Ligations were checked by restriction enzyme digestion and confirmed by PCR analysis using 1μg plasmid DNA and 0.3μl dream taq polymerase (for primers see Table 3). All constructed plasmids were sequenced for verification (Macrogen, Amsterdam, Netherlands).

ACKNOWLEDGMENTS

We would like to thank Omid Karami for providing tulip explants and related information about tulip tissue culture, Ivo Gariboldi for help in making the constructs, Muhammad Ibrahim for helping with statistical analysis, Ward de Winter for help with plant media and plant growth and Gerda Lamers for the assistance with microscopy and staining of plant material.

Table 2. List of binary vectors used for *Agrobacterium* infiltration.

Name	Properties	Source
pSDM6500 [*pvirF::GFP$_{11}$-L$_2$-dvirF*]	pSDM3760 backbone with the coding sequence of *GFP$_{11}$-L2-dvirF* under control of the *virF* promoter (*L2* is the linker sequence having multiple unique restriction sites).	Chapter 3
pSDM6503[*pvirF::GFP$_{11}$-AHL15- ΔvirF*]	pSDM3760 backbone with the *GFP$_{11}$-AHL15-ΔvirF* coding sequence under control of the *virF* promoter	Chapter 3
pSDM6504[*pvirF::GFP$_{11}$-BBM- ΔvirF*]	pSDM3760 backbone with the *GFP$_{11}$-BBM-ΔvirF* coding sequence under control of the *virF* promoter	Chapter 3
pSDM3764[*35S::GFP$_{1-10}$*]	pCambia1302 with *GFP$_{1-10}$* coding sequence under control of the *35S* promoter and the *CaMV* terminator.	(Sakalis et al., 2014)
pSDM6506[*35S::GFP(i)*]	pCambia1302 with *GFP(i)* coding sequence under control of the *35S* promoter and the *CaMV* terminator.	This study
pSDM6507[*35S::NLS-GFP(i)*]	pCambia1302 with *NLS-GFP(i)* coding sequence under control of the *35S* promoter and the *CaMV* terminator.	This study
pSDM6505[*35S::pGFP(i)*]	pCambia1302 with the *pGFP $_{1-11}$(i)* coding region under control of the *35S* promoter and the *CaMV* terminator.	This study
pSDM6508[*35S::GFP$_{1-10}$(i)*]	pCambia1302 with the *GFP$_{1-10}$(i)* coding region under control of the *35S* promoter and the *CaMV* terminator.	This study
pSDM6509[*35S::NLS-GFP$_{1-10}$(i)*]	pCambia1302 with *NLS-GFP$_{1-10}$(i)* coding region under control of the *35S* promoter and the *CaMV* terminator.	This study
pSDM6514 [*35S::NLS-GFP$_{1-10}$(i)-pvirF::GFP$_{11}$-L2- ΔvirF*]	pCambia1302 with *NLS-GFP$_{1-10}$(i)* coding region under control of the 35S promoter and the CaMV terminator and pSDM3760 backbone with *GFP$_{11}$-L2-ΔvirF* coding sequence under control of the *virF* promoter. (*L2* is the linker sequence having multiple unique restriction sites).	This study
pEX-A2[*GFP$_{1-10}$(i)*]	*GFP$_{1-10}$(i)* coding sequence	Eurofins
pEX-A2[*NLS-GFP$_{1-10}$(i)*]	*NLS-GFP$_{1-10}$(i)* coding sequence	Eurofins

Table 3. List of primers used in this study

Primer name	Sequence (5' → 3')
XbaI-GFP1-10 Fw	GCTCTAGAATGGTTTCGAAAGGCGA
XbaI-GFP1-10 Rv	CCCTCGAGTTATTTCTCGTTTGGGT
NcoI-GFP_{1-10}-Fw	GCCCATGGTTTCGAAAGGCGAGGA
BstEII-GFP_{1-10}-Rev	GGGTCACCTTATTTCTCGTTTGGGTCTT
Plant GFP Fw	CGAGAATATTCGGATCCCATGGGCAA
Plant GFP Rev	TGAATTCGCTGCAGGTCACCTCACTT
pEX-A2-Fw	GGAGCAGACAAGCCCGTCAGG
pEX-A2-Rev	GCCGGAAGCATAAAGTGTAAAGCCTG
FW GFP1-11nls	TCATTTGGAGAGAACACGGGGG
Rev GFP1-11nls	GGAAATTCGAGCTGGTCACCTTA
35Sgfp11-dVirF-Fr	TCATTTGGAGAGAACACGGG
35Sgfp11-dVirF-Rv	TAATCATCGCAAGACCGGCA

REFERENCES

1. **Baltes NJ, Gil-Humanes J, Cermak T, Atkins PA, Voytas DF** (2014) DNA replicons for plant genome engineering. Plant Cell 26: 151–163
2. **Barampuram S, Zhang ZJ** (2011) Recent advances in plant transformation. Methods Mol Biol 701: 1–35
3. **Beijersbergen A, Dulk-Ras AD, Schilperoort RA, Hooykaas PJJ** (1992) Conjugative transfer by the virulence system of *Agrobacterium tumefaciens*. Science 256: 1324–1327
4. **Bethesda Research Laboratories** (1986) *E. coli* DH5 alpha competent cells. Focus - Bethesda Res Lab 8: 9
5. **Bibi Y, Zia M, Nisa S, Habib D, Waheed A, Chaudhary FM** (2011) Regeneration of *Centella asiatica* plants from non-embryogenic cell lines and evaluation of antibacterial and antifungal properties of regenerated calli and plants. J Biol Eng 5: 13
6. **Cabantous S, Terwilliger TC, Waldo GS** (2005) Protein tagging and detection with engineered self-assembling fragments of green fluorescent protein. Nat Biotechnol 23: 102–107
7. **Chandran Darbari V, Waksman G** (2015) Structural biology of bacterial type IV secretion systems. Annu Rev Biochem 84: 603–29
8. **den Dulk-Ras A, Hooykaas PJJ** (1995) Electroporation of *Agrobacterium tumefaciens*. Methods Mol Biol 55: 63–72
9. **Gelvin SB** (2006) *Agrobacterium* virulence gene induction. Methods Mol Biol 343: 77–84
10. **Heidmann I, de Lange B, Lambalk J, Angenent GC, Boutilier K** (2011) Efficient sweet pepper transformation mediated by the BABY BOOM transcription factor. Plant Cell Rep 30: 1107–1115
11. **Jin S, Prusti RK, Roitsch T, Ankenbauer RG, Nester EW** (1990) Phosphorylation of the VirG protein of *Agrobacterium tumefaciens* by the autophosphorylated VirA protein: Essential role in biological activity of VirG. J Bacteriol 172: 4945–4950
12. **Jin SG, Komari T, Gordon MP, Nester EW** (1987) Genes responsible for the supervirulence phenotype of *Agrobacterium tumefaciens* A281. J Bacteriol 169: 4417–4425
13. **Kothari SL, Joshi A, Kachhwaha S, Ochoa-Alejo N** (2010) Chilli peppers - A review on tissue culture and transgenesis. Biotechnol Adv 28: 35–48
14. **Kumar RB, Das A** (2002) Polar location and functional domains of the *Agrobacterium tumefaciens* DNA transfer protein VirD4. Mol Microbiol 43: 1523–1532
15. **Lacroix B, Citovsky V** (2013) The roles of bacterial and host plant factors in *Agrobacterium*-mediated genetic transformation. Int J Dev Biol 57: 467–481
16. **Lacroix B, Li J, Tzfira T, Citovsky V** (2006) Will you let me use your nucleus? How *Agrobacterium* gets its T-DNA expressed in the host plant cell. Can J Physiol Pharmacol 84: 333–345
17. **Lai EM, Kado CI** (2000) The T-pilus of *Agrobacterium tumefaciens*. Trends Microbiol 8: 361–369
18. **Lazo GR, Stein PA, Ludwig RA** (1991) A DNA transformation-competent *Arabidopsis* genomic library in *Agrobacterium*. Biotechnology **9**: 963–967
19. **Li X, Yang Q, Tu H, Lim Z, Pan SQ** (2014) Direct visualization of *Agrobacterium*-delivered VirE2 in recipient cells. Plant J 77: 487–495
20. **McCormac AC, Elliott MC, Chen DF** (1998) A simple method for the production of highly competent cells of *Agrobacterium* for transformation via electroporation. Mol Biotechnol **9**: 155–159
21. **Melchers LS, Regensburg-Tuïnk TJ, Bourret RB, Sedee NJ, Schilperoort RA, Hooykaas PJJ** (1989) Membrane topology and functional analysis of the sensory protein VirA of *Agrobacterium tumefaciens*. EMBO J 8: 1919–1925

22. **Mersereau M, Pazour GJ, Das A** (1990) Efficient transformation of *Agrobacterium tumefaciens* by electroporation. Gene 90: 149–151

23. **Pang SZ, DeBoer DL, Wan Y, Ye G, Layton JG, Neher MK, Armstrong CL, Fry JE, Hinchee MA, Fromm ME** (1996) An improved green fluorescent protein gene as a vital marker in plants. Plant Physiol 112: 893–900

24. **Podwyszyńska M, Sochacki D** (2010) Micropropagation of tulip: production of virus-free stock plants. Methods Mol Biol 589: 243–256

25. **Rossi L, Hohn B, Tinland B** (1996) Integration of complete transferred DNA units is dependent on the activity of virulence E2 protein of *Agrobacterium tumefaciens*. Proc Natl Acad Sci USA 93: 126–130

26. **Sakalis PA, van Heusden GPH, Hooykaas PJJ** (2014) Visualization of VirE2 protein translocation by the *Agrobacterium* type IV secretion system into host cells. Microbiol Open 3: 104–117

27. **Schrammeijer B, den Dulk-Ras A, Vergunst AC, Jácome EJ, Hooykaas PJJ** (2003) Analysis of Vir protein translocation from *Agrobacterium tumefaciens* using *Saccharomyces cerevisiae* as a model: Evidence for transport of a novel effector protein VirE3. Nucleic Acids Res 31: 860–868

28. **Stachel SE, Messens E, Van Montagu M, Zambryski P** (1985) Identification of the signal molecules produced by wounded plant cells that activate T-DNA transfer in *Agrobacterium tumefaciens*. Nature 318: 624–629

29. **Subramoni S, Nathoo N, Klimov E, Yuan Z-C** (2014) *Agrobacterium tumefaciens* responses to plant-derived signaling molecules. Front Plant Sci 5: 322

30. **van Engelenburg SB, Palmer AE** (2010) Imaging type-III secretion reveals dynamics and spatial segregation of Salmonella effectors. Nat Methods 7: 325–30

31. **van Larebeke N, Engler G, Holsters M, van Den Elsacker S, Zaenen I, Schilperoort RA, Schell J** (1974) Large plasmid in *Agrobacterium tumefaciens* essential for crown gall-inducing ability. Nature 252: 169–170

32. **Vergunst AC, Schrammeijer B, den Dulk-Ras A, de Vlaam CM, Regensburg-Tuïnk TJ, Hooykaas PJJ** (2000) VirB/D4-dependent protein translocation from *Agrobacterium* into plant cells. Science 290: 979–82

33. **Vergunst AC, van Lier MCM, den Dulk-Ras A, Stüve TAG, Ouwehand A, Hooykaas PJJ** (2005) Positive charge is an important feature of the C-terminal transport signal of the VirB/D4-translocated proteins of *Agrobacterium*. Proc Natl Acad Sci USA 102: 832–7

34. **Vogel AM, Das A** (1992) Mutational analysis of *Agrobacterium tumefaciens* virD2: Tyrosine 29 is essential for endonuclease activity. J Bacteriol 174: 303–308

35. **Wang K, Stachel SE, Timmerman B, Van Montagu M, Zambryski PC** (1987) Site-specific nick in the T-DNA border sequence as a result of *Agrobacterium* vir gene expression. Science (80-) 235: 587–591

36. **Wilmink A., van de Ven BCE, Dons JJM** (1992) Expression of the GUS-gene in the monocot tulip after introduction by particle bombardment and *Agrobacterium*. Plant Cell Rep 11: 76–80

37. **Wroblewski T, Tomczak A, Michelmore R** (2005) Optimization of *Agrobacterium*-mediated transient assays of gene expression in lettuce, tomato and *Arabidopsis*. Plant Biotechnol J 3: 259–273

38. **Zaenen I, van Larebeke N, Teuchy H, van Montagu M, Schell J** (1974) Supercoiled circular DNA in crown-gall inducing *Agrobacterium* strains. J Mol Biol. doi: 10.1016/S0022-2836(74)80011-2

39. **Ziemienowicz A** (2014) *Agrobacterium*-mediated plant transformation: Factors, applications and recent advances. Biocatal Agric Biotechnol 3: 95–102

40. **Zupan J, Hackworth CA, Aguilar J, Ward D, Zambryski P** (2007) VirB1 promotes T-pilus formation in the vir-type IV secretion system of *Agrobacterium tumefaciens*. J Bacteriol 189: 6551–6563

SUPPLEMENTARY FIGURES

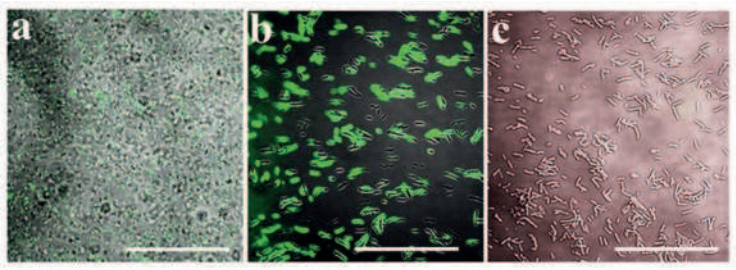

Figure S1. An intron in the *GFP*$_{1-10}$ coding sequence effectively prevents bacterial GFP expression in the generic split-GFP system. a,b) Confocal images of *Agrobacterium tumefaciens* strain AGL1 containing *p35S::GFP*$_{1-10}$ and *pVirF::GFP*$_{11}$*-dVirF* after overnight induction with acetosyringone (a) and after co-cultivation with *N. tabacum* leaf discs (b). c) Confocal images of *Agrobacterium tumefaciens* strain AGL1 containing *p35S::GFP*$_{1-10}$*(i)* and *pVirF::GFP*$_{11}$*-dVirF* where the *GFP*$_{1-10}$ coding region is disrupted by an intron *(i)*. Shown are merged images of the GFP channel and the transmitted light channel. Scale bar is 10 µm.

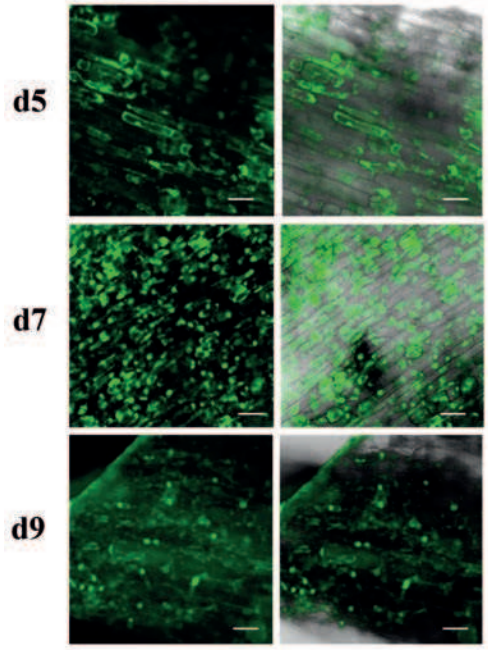

Figure S2. AMPT to tulip cells peaks after 7 days of cocultivation with *Agrobacterium*. a-c) Confocal images of *in vitro* regenerated shoot tissues (from tulip bulb stem explants) cocultivated with *Agrobacterium tumefaciens* strain AGL1 containing *p35S::GFP*$_{1-10}$*(i)* and *pVirF::GFP*$_{11}$*-dVirF* and cocultivated for 5 (a), 7 (b) or 9 days (c) on hormone free medium. Left panel shows the GFP channel, right panel shows a merged image of the GFP channel and the transmitted light channel. Scale bar is 0.1 µm.

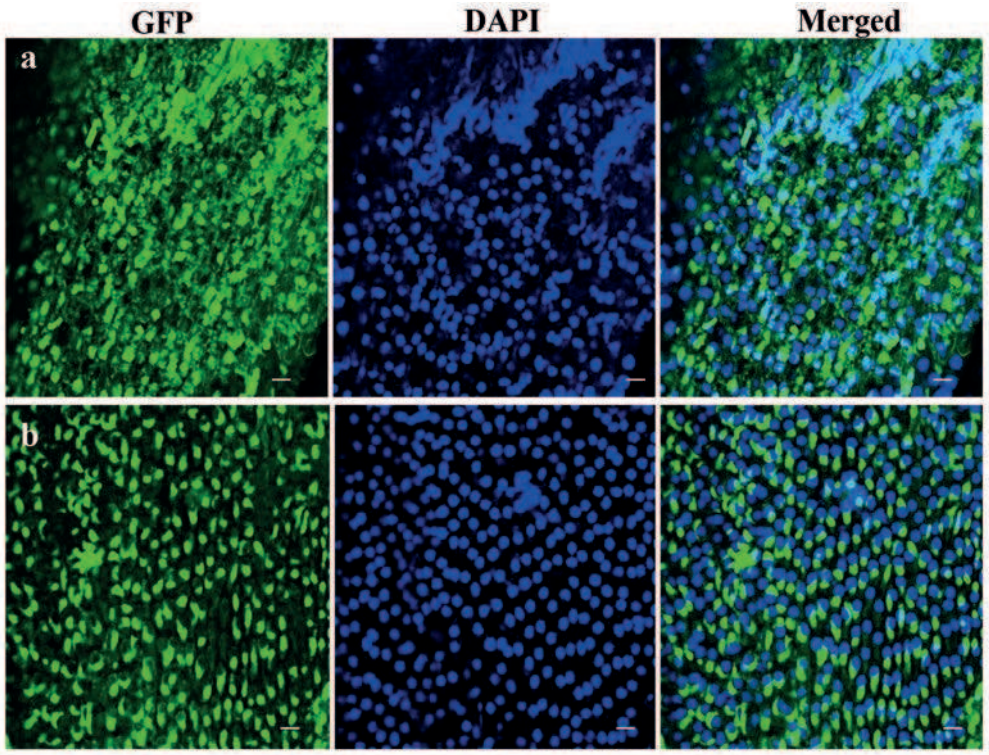

Figure S3. DAPI staining confirms nuclear GFP fluorescence in tulip cells after AMPT or AMT. a,b) Confocal laser scanning microscopy images of DAPI stained tulip tissues shown in figure 5 after cocultivation for 7 days with *Agrobacterium* strain AGL1 containing *p35S::GFP*$_{1\text{-}10}$*(i)* and *pVirF::GFP*$_{11}$*-dVirF* (a) or with strain AGL1 *35S::NLS-GFP(i)* and subsequent regeneration for 4-5 weeks (b). Left panel shows GFP channel, middle panel shows DAPI stained nuclei in blue channel, and the right panel shows a merged image of the GFP and DAPI channels. Scale bar is 0.1mm.

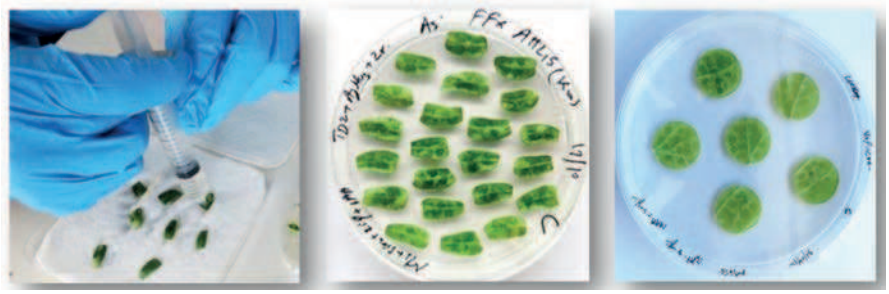

Figure S4. Syringe infiltration method of sterile *Capsicum annum* cotyledons (left and middle panel) or *Nicotiana tabacum* leaf discs (right panel).

Appendix 1. a,b) DNA sequences of the original GFP (*GFP(i)*) (a) and the plant-optimized GFP (*pGFP(i)*) (b) showing the inserted intron (i) sequence in red. c) Alignment of *GFP(i)* sequence with *pGFP(i)* sequence shows intron position and DNA sequence differences.

a). Full length $GFP_{1\text{-}10+11}$(i) (GFP(i)); intron sequence is RED and underlined

ATGGTTTCGAAAGGCGAGGAGCTGTTCACAGGCGTGGTGCCAATCCTGGTGGAGCT
GGACGGCGACGTGAACGGCCACAAATTCAGCGTGAGAGGCGAGGGCGAGGG
CGACGCCACAATCGGCAAACTGACACTGAAATTCATCTGCACAACAGGCAAACTGC
CAGTGCCCTGGCCAACACTAGTGACAACACTGACATACGGCGTGCAGTGCTTCAG
CAGATATCCGGACCACATGAAAAGACACGACTTCTTCAAAAGCGCCATGCCAGAG
GGCTACGTGCAGGAGAGAACAATCAGCTTCAAAGACGACGGCAAATACAAAA
CAAGAGCCGTGGTGAAATTCGAGGGCGACACACTGGTGAACAGAATCGAGCT
GAAG**GTATGACAATTTACTCGAACTTCCTTTTTTAACTCGAACTATGTATATACA**
CAACAACGTTAATAATTAAGTCGTACTCATTTTGAATCTACTGACTCTAGATCCT
GATTCACACATGTAATATAATTGCAGGGCACAGACTTCAAAGAGGACGGCAA
CATCCTGGGCCACAAACTGGAGTACAACTTCAACAGCCACAACGTGTACATCA
CAGCCAACAAACAGAAAAACGGCATCAAAGCCAACTTCACAGTGAGACACAACGT
GGAGGACGGCAGCGTGCAGCTCGCCGACCACTACCAGCAGAACACACCAATCGG
CGACGGCCCAGTGCTGCTGCCAGACAACCACTACCTGAGCACACAGACAGTGCT
GAGCAAAGACCCAAACGAGAAACGGGACCACATGGTGCTGCACGAGTACGT
GAACGCCGCCGGCATCACATAA

b). Full length plant enhanced $pGFP_{1\text{-}11}$ (pGFP(i)) ; intron sequence is RED and underlined

ATGGGCAAGGGCGAGGAACTGTTCACTGGCGTGGTCCCAATCCTGGTGGAACTG
GATGGTGATGTGAACGGGCACAAGTTCTCCGTCAGCGGAGAGGGTGAA
GGTGATGCCACCTACGGAAAGCTCACCCTGAAGTTCATCTGCACTACCG
GAAAGCTCCCTGTTCCGTGGCCAACCCTCGTCACCACTTTCACCTACGGTGT
TCAGTGCTTCTCCCGGTACCCAGATCACATGAAGCAGCATGACTTCTTCAAGAG
CGCCATGCCCGAAGGCTACGTGCAAGAAAGGACTATCTTCTTCAAGGATGACGG
GAACTACAAGACACGTGCCGAAGTCAAGTTCGAAGGTGATACCCTGGTGAACCG
CATCGAGCTGAAAG**GTATGACAATTTACTCGAACTTCCTTTTTTAACTCGAAC**
TATGTATATACACAACAACGTTAATAATTAAGTCGTACTCATTTTGAATCTACT
GACTCTAGATCCTGATTCACACATGTAATATAATTGCAGGCATCGATTTCAAG
GAAGATGGAAACATCCTCGGACACAAGCTGGAGTACAACTACAACTCCCACAACG
TATACATCATGGCCGACAAGCAGAAGAACGGCATCAAGGTGAACTTCAAGAT
CAGGCACAACATCGAAGATGGAAGCGTGCAACTGGCGGACCACTACCAGCAGAA
CACGCCCATCGGCGATGGCCCTGTCCTGCTGCCGGACAACCATTACCTGTCCACG
CAATCTGCCCTCTCCAAGGACCCCAACGAGAAGAGGGACCACATGGTCCTGCTG
GAGTTCGTGACGGCTGCTGGGATCACGCATGGCATGGATGAACTCTACAAGTGA

c).

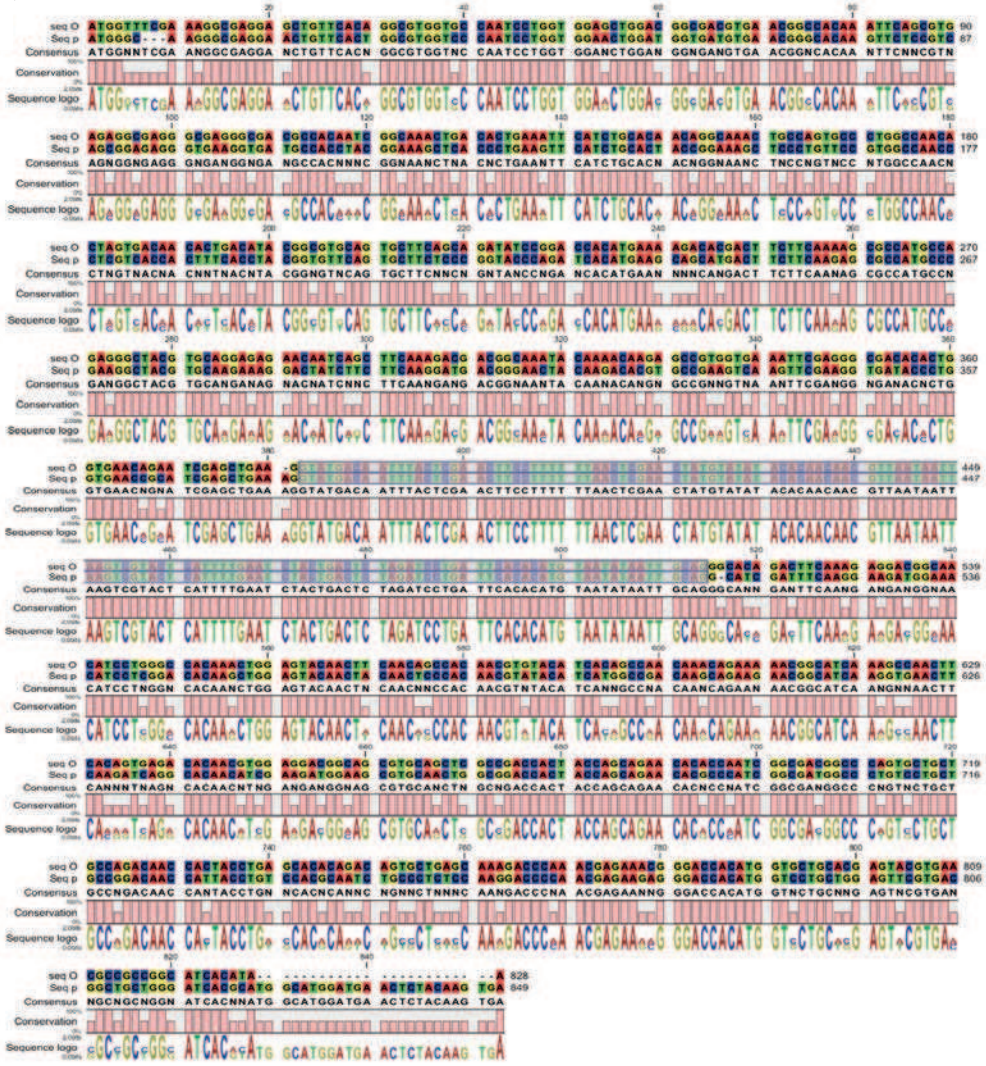

Appendix 2. a,b) DNA sequences of *GFP$_{1-10}$(i)* (a) and *NLS-GFP$_{1-10}$(i)* (b) showing inserted intron in red and the nuclear localization signal (NLS) in purple. c) Alignment of *GFP$_{1-10}$(i)* with *NLS-GFP$_{1-10}$(i)* sequence shows intron and NLS positions and DNA sequence differences.

a). GFP$_{1-10}$(i); intron sequence is RED and underlined.

ATGGTTTCGAAAGGCGAGGAGCTGTTCACAGGCGTGGTGCCAATCCTGGTGGAGCT
GGACGGCGACGTGAACGGCCACAAATTCAGCGTGAGAGGCGAGGGCGAGGG
CGACGCCACAATCGGCAAACTGACACTGAAATTCATCTGCACAACAGGCAAACTGC
CAGTGCCCTGGCCAACACTAGTGACAACACTGACATACGGCGTGCAGTGCTTCAG
CAGATATCCGGACCACATGAAAAGACACGACTTCTTCAAAAGCGCCATGCCAGAG
GGCTACGTGCAGGAGAGAACAATCAGCTTCAAAGACGACGGCAAATACAAAACAA
GAGCCGTGGTGAAATTCGAGGGCGACACACTGGTGAACAGAATCGAGCTGAAA
G**GTATGACAATTTACTCGAACTTCCTTTTTTAACTCGAACTATGTATATACACAA
CAACGTTAATAATTAAGTCGTACTCATTTTGAATCTACTGACTCTAGATCCTGAT
TCACACATGTAATATAATTGCAG**GCACAGACTTCAAAGAGGACGGCAACATCCT
GGGCCACAAACTGGAGTACAACTTCAACAGCCACAACGTGTACATCACAGC
CAACAAACAGAAAAACGGCATCAAAGCCAACTTCACAGTGAGACACAACGTG
GAGGACGGCAGCGTGCAGCTCGCCGACCACTACCAGCAGAACACACCAATCGG
CGACGGCCCAGTGCTGCTGCCAGACAACCACTACCTGAGCACACAGACAGTGCT
GAGCAAAGACCCAAACGAGAAATAA

b). NLS:GFP$_{1-10}$(i); NLS is purple and intron sequence is RED and underlined.

ATGGAGCCTCCTAAGAAGAAGAGGAAGGTTGAGCTGATGGTTTCGAAAGGC
GAGGAGCTGTTCACAGGCGTGGTGCCAATCCTGGTGGAGCTGGACGGCGACGT
GAACGGCCACAAATTCAGCGTGAGAGGCGAGGGCGAGGGCGACGCCACAATCGG
CAAACTGACACTGAAATTCATCTGCACAACAGGCAAACTGCCAGTGCCCTGGC
CAACACTAGTGACAACACTGACATACGGCGTGCAGTGCTTCAGCAGATATCCG
GACCACATGAAAAGACACGACTTCTTCAAAAGCGCCATGCCAGAGGGCTACGTG
CAGGAGAGAACAATCAGCTTCAAAGACGACGGCAAATACAAAACAAGAGCCGT
GGTGAAATTCGAGGGCGACACACTGGTGAACAGAATCGAGCTGAAAG**GTATGA
CAATTTACTCGAACTTCCTTTTTTAACTCGAACTATGTATATACACAACAACGT
TAATAATTAAGTCGTACTCATTTTGAATCTACTGACTCTAGATCCTGATTCA
CACATGTAATATAATTGCAG**GCACAGACTTCAAAGAGGACGGCAACATCCTG
GGCCACAAACTGGAGTACAACTTCAACAGCCACAACGTGTACATCACAGCCAA
CAAACAGAAAAACGGCATCAAAGCCAACTTCACAGTGAGACACAACGTGGAG
GACGGCAGCGTGCAGCTCGCCGACCACTACCAGCAGAACACACCAATCGG
CGACGGCCCAGTGCTGCTGCCAGACAACCACTACCTGAGCACACAGACAGTGCT
GAGCAAAGACCCAAACGAGAAATAA

c).

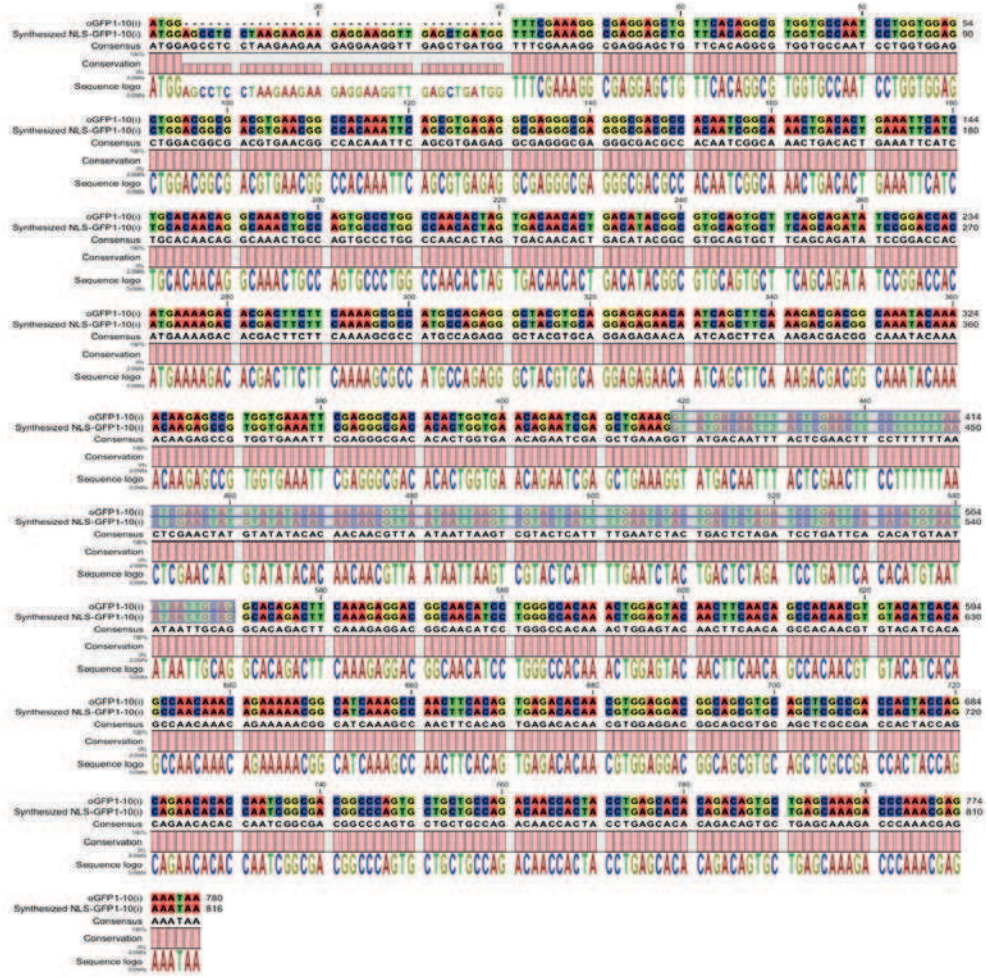
oGFP1-10(i)
Synthesized NLS-GFP1-10(i)
Consensus
Conservation
Sequence logo